Computational Studies of the Medically Relevant Enzyme Tripeptidyl Peptidase-1 (TPP1) and Kumamolisin-As (Kum-As)

Mauricio Valenzuela
College Scholars in Biochemistry, Chemistry and Computational Biology
Mentor: Dr. Hong Guo
University of Tennessee-Knoxville
Knoxville, Tennessee
April 2009

INDEX

I. Introduction 3

(i) Sedolisin Family of Enzymes and Their Structures ……3

(ii) Neuronal Lipoid Fuscinosis……..……7

II. Computational Studies of TPP1 10

(i) Methods……...10

(ii) Results……..11

(iii) Discussion……...….13

III. Computational Studies of Kum-As 14

(i) Methods……...16

(ii) Results and Discussion……....17

Conclusion 19

Acknowledgements 20

References 21

I. Introduction

(i) Sedolisin Family of Enzymes and Their Structures

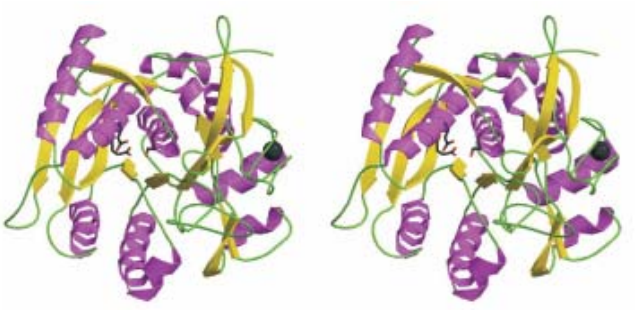
Proteolytic enzymes (peptidases, proteinases or proteases) catalyze the cleavage of peptide bonds and form one of the largest and very important groups of enzymes. Sedolisins, also known as serine-carboxyl peptidases, are members of the MEROPS family of peptidades, S53 proteolytic enzymes. Their fold resembles that of subtilisin; however, they are considerably larger than subtilisin, with the mature catalytic domains containing approximately 375 amino acids.[1] Other common properties among sedolisins include the lack of inhibition by pepstatin, stabilization by a Ca^{2+}, and presence of conserved acidic residues required for the activity.

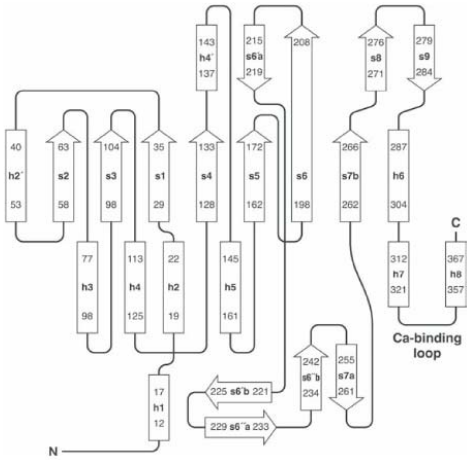
Structural comparison for two members of the family of serine-carboxyl peptidases, sedolisin (PSCP)[2, 3] and kumamolisin (KSCP)[4] based on published crystal structures shows that the three-dimensional fold of sedolisin (PSCP) contains a 7-stranded, all-parallel β sheet (strands s2-s3-s1-s4-s5-s6-s7b). This β sheet is flanked on the both sides by several helices (Fig. 1A,B).[1] In addition, the fold of sedolisin contains several additional shorter strands and helices, with three pairs of strands (s8-s9, s6`b-s6``a, and s6``b-s7a) forming β hairpins on the surface of the proteins. Helix h2 is absent in kumamolisin, whereas an additional short strand (s1a), absent in sedolisin, is observed in kumamolisin.[4] The core of kumamolisin consists of a highly twisted β sheet, flanked by five helices on both sides, composed of eight parallel β strands arranged in the sequential order s2, s3, s1, s4, s5, s6, s7, and s11 (Fig. 1C).[4] The differences in the structures of sedolisin and kumamolisin are mainly limited to the surface areas, while the cores of both enzymes are rather similar.[1] Both sedolisin and

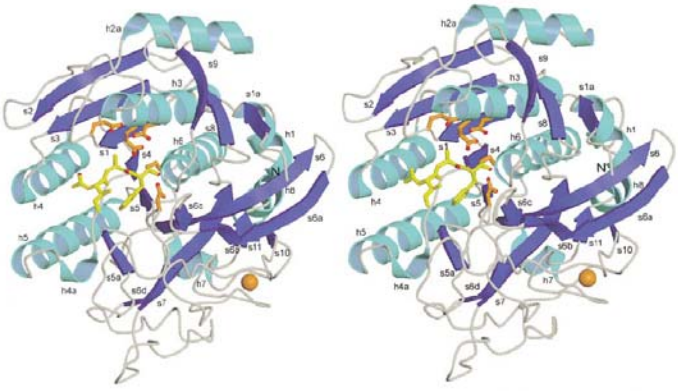
kumamolisin have a Ca^{+2} binding site that seems to be in similar positions in all structures of the family reported so far. The structural role of this site in sedolisin seems to tie the long loop containing residues 328–342 to a short loop, 343–348, and both of them to opposite strands around residue 353; experiments about this site suggest the importance of the integrity of the Ca^{+2} binding site for the activity of the enzyme.[1]

Serine-carboxyl peptidases have maximum activity at low pH. One possible reason for this behavior is that a key Asp residue (e.g., Asp170 in sedolisin and Asp164 in kumamolisin) would need to be protonated in order to serve its function;[1] as a consequence, this event is favored at higher concentration of H^{+}. The active site of serine-carboxyl peptidases contains a unique catalytic triad Ser-Glu-Asp (SED in the single letter code) that differs from classical serine proteases. Details of catalytic mechanisms, substrate specificities and the role of the active-site residues are still poorly understood for this sedolisin family of enzymes.

One of the important members of the sedolisin family is tripeptidyl peptidase-1 (TPP1), which represents the only known mammalian member of the sedolisin family. As discussed before, this group of enzymes is characterized by a subtilisin-like fold, the Ser-Glu-Asp catalytic triad and maximum enzymatic activity at low pH. A mutation in the CLN2 gene that encodes for this protein (TPP1) may cause a fatal neurodegenerative disease of childhood known as late infantile neuronal ceroid lipofuscinosis. The gene product is initially synthesized as an inactive proenzyme that is autocatalytically converted to an active form.[5]




143
h4'
137
215
s6'a
219
208
276
s8
271
279
s9
284
40
h2'
53
63
s2
58
104
s3
98
35
s1
29
133
s4
128
172
s5
162
s6
198
266
s7b
262
287
h6
304
C
77
h3
98
113
h4
125
22
h2
19
145
h5
161
312
h7
321
367
h8
357
Ca-binding
loop
242
s6''b
234
255
s7a
261
17
h1
12
225 s6'b 221
229 s6''a 233
N



The crystal structures for the proform of TPP1 were recently solved at 1.85 Å and 2.35 Å resolution, respectively.[6, 7] X-ray crystallographic analysis reveals a globular structure with a subtilisin-like fold, a S475-E272-D276 catalytic triad and an octahedrally coordinated Ca^{2+} binding site which are all characteristic features of the S53 sedolisin family of peptidases.[7] Chemical modification studies of TPP1 have revealed that S475 is the active-site nucleophile.[5]

TPP1 has a primary tripeptidyl exopeptidase activity with a pH optimum of ~5.0 and catalyzes the sequential release of tripeptides from the unsubstituted N-termini of substrates.[6] An example of this tripeptidyl exopeptidase activity is when TPP1 releases Gly-Pro-X triplets from synthetic collagen-like polymers, suggesting that it may be involved in part of the pathway leading to the degradation of the bone matrix proteins or bone resorption.[8] The acidic pH optimum suggests that TPP1 has a lysosomal localization, and experimental data show that this enzyme is inhibited by reagents that modify serine and histine residues.[8] The mechanism for activity of TPP1 to release tripeptides is still poorly understood, but recent studies suggest that a kind of 'molecular ruler' in the enzyme, which ensures the mechanism that removes tripeptides and not longer or shorter fragments, with the positively charged N-terminal amino group being the essential determinant for this activity.[9] Another example of this molecular ruler mechanism is observed in the role of Glu-331 and Glu-305 in substrate binding of tripeptidyl-peptidase II.[9]

TPP1 is the eukaryotic homolog of the prokaryotic kumamolisin. Because of these similarities, the study of kumamolisin (or kumamolisin-As, which has over 90% sequence identity with kumamolisin) could provide more clues to better understand the chemical basis of the neuronal disease. In this thesis, two reported X-ray crystal structures of TPP1 are

examined to better understand the acylation reaction. Molecular dynamics simulations are performed to understand the dynamic nature of the key amino-acids in the active site, the solvent and the peptide substrate.

(ii) Neuronal Lipoid Fuscinosis

The neuronal ceroid lipofuscinoses (NCLs) are a group of related hereditary neurodegenerative disorders in which there is an accumulation of autofluorescent lysosome-like bodies in the neurons and other cells and that occur at a frequency of between 2 and 4 in 100000 live births.[10, 11] Absence of TPP1 results in lysosomal storage with an accompanying axonal degeneration throughout the central nervous system (CNS), which leads to this progressive neurodegeneration and early death.[12]

Diagnosis is based on problems with vision, behavioral changes and seizures. All childhood forms are eventually fatal. There is no effective treatment for NCL, and progression is reflected by a decline in mental abilities, increasingly severe and untreatable seizures, blindness and loss of motor skills.[13] This lysosomal storage disease of childhood typically presents between the ages of 2 and 4 years with the onset of seizures.[6] However, enzyme and gene therapy are promising approaches that will be discussed in this senior thesis. Both of them could rescue TPP1 activity and prevent or slow disease progression.

Risk Factors, Pathology and Clinical Factors

According to a 2006 pediatric neurology online article by Celia Chang,[14] the neuronal ceroid lipofuscinosis, also known as Baten Disease, are the most common of the neurogenetic storage diseases with a prevalence of 1 in 12.500 in some populations. Seizure, dementia, visual loss and cerebral atrophy are some examples of the progressive symptoms.

Batten made the first clinicopathologic correlation in 1903 and pointed out the differences from Tay–Sachs disease. Pathophysiology studies show that patients with CLN2 mutated gene are deficient in TPP1 enzyme, which is in charge of removing tripeptides from the N-terminal of polypeptides. More than fifty-two mutations have been reported in all 13 exons of the CLN2 gene. A recent study have reported the currently known pathogenic mutations on the TPP1 structure (Fig. 2).[7]

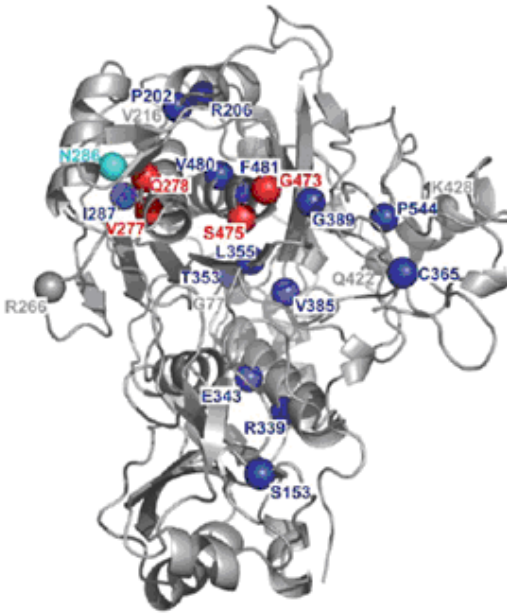


Fig.2. Pathogenic TPP1 missense mutations mapped onto the TPP1 structure as labeled spheres. Mutations compromising the catalytic activity, conformational destabilization and unclear structural consequences are represented as red, blue and gray colored spheres, respectively. Pal *et al.* 2008

Patients with NCL have short life expectancy; how short depends on the type of NCL. In the US approximately 25,000 families are affected with a form of NCL. In the particular type CLN2, the worldwide prevalence is 0.6–0.7 per million inhabitants, with an incidence of 0.46 per 1.000.000 live births.[14]

Clinical differences are important to properly identify the type of NCL. As previously mentioned, the deficiency in TPP1, which is the focus of this thesis, is related

with the CLN2 or Jansky–Bielschowsky type or late infantile neuronal ceroid lipofuscinosis (LINCL). The other types includes the CLN1 or Santavuori–Haltia type or infantile NCL, the CLN3 or Spielmeyer–Sjogren type or adult NCL, the CLN4 or Kufs disease or adult NCL, the CLNS or Finnish Variant late infantile NCL, the CLN6 or Variant late infantile/early juvenile NCL, the CLN7 or Turkish variant late infantile NCL, the CLN8 or Turkish variant late infantile NCL and Northern epilepsy.[14]

Laboratories studies are useful to diagnose the disease. For the CNL2 type, the levels of TPP1 in leukocytes, cultured fibroblasts, dried blood spots, and saliva can be measured and then compared to normal levels. For instance, fibroblast TPP1 activity is approximately 17.000 micromoles of amino acids produced per hour per mg. of protein, while the activity of TPP1 in LICNL is less than 4% of normal. In addition, other biochemical abnormalities can be detected such as the ATP synthase complex subunit C accumulation in lysosomes of patients. Other applicable types of tests are DNA testing and electron microscopy ultrastructural findings.[14]

Current Treatment/Therapies

Currently there is no treatment of demonstrated efficacy for the late infantile neuronal ceroid lipofuscinosis (LINCL), but some advances are being made in some fields. Proof-of-principle for a viral-mediated gene therapy has been established in a mouse model of LINCL, with a significant improvement in disease phenotype achieved with the use of adeno-associated virus (AAV) vectors expressing TPP1. The results emphasize the importance of early intervention for enhanced therapeutic benefit, which may provide guidance in designing novel treatment strategies for LINCL patients.[6, 12] Recently AAV vectors has been used as part of the therapy for affected children. Although the clinical

benefits are still under study, this trial was not matched, randomized, or blinded and lacked a placebo control group. Assessment of the primary outcome variable suggests a slowing of progression of LINCL in the treated children.[15] Enzyme replacement therapy is another approach that was already successful with other lysosomal storage diseases and that is currently being investigated in LINCL.[6] Purified recombinant human TPP1 that contains the mannose 6-phosphate lysosomal targeting modification can be taken up by LINCL fibroblasts were it degrades storage material, and the protein has been introduced into the cerebrospinal fluid of the LINCL mouse model via intraventricular injection. This infusion of recombinant human TPP1 through an intraventricular cannula led to enzyme distribution in several regions of the brain of treated mice, resulting in significant uptake into the brain and some correction of neuropathology.[6, 16]

II. Computational Studies of Tripeptidyl Peptidase-1 (TPP1)

(i) Methods

The X-ray crystal structures of the enzyme studied, TPP1, were obtained from the Protein Data Bank (PDB ID: 3ee6 and 3edy). Both structures were superimposed using MOE 2007 software to construct a model that contains the five amino acid peptide of the linker fragment (Gly-Pro-Hsp-Phe-Phe). Hydrogen atoms and water molecules were added using MOE. The key amino acids surrounding the five amino acid peptide to a distance of 4.5 Å were selected with the rest of the system fixed (in order to focus only on the desired area for study). Energy minimization with a gradient of 0.00001 was performed on the model, and CHARMM22 was used as the force field. Molecular dynamics simulations were

performed for 4000 steps (4ns) with 0.002ps time step and the temperature of 300 K. The root-mean-square deviation (RMSD) compares the position of atoms before and after the dynamics simulations. Once the 4-ns dynamic simulation ended, the RMSD values of the key amino acids and the substrate were plotted and compared.

(ii) Results

The TPP1 model analyzed by MOE reveals all the features discussed above. The analysis of the elements of secondary structure for this enzyme reveals the number of β-strands and α-helices already described in the introduction (Fig.3A). The catalytic triad (Fig.3B) and the five amino acid link peptide (Fig.3C) reveal a series of H-bonding interactions between Ash276-Glu272 (two hydrogen bonds), Ser475-Hsp3, and Phe4-Pro2 before the dynamic simulations (Fig. 3C).

After 4-ns molecular dynamic simulations, the average conformations of the residues from the catalytic triad, Asp360 and the substrate have new hydrogen-bonding interactions between Ash360-Hsp3, Ser475-Gly1, and Ash276-Glu272. Ash represents the protonated Asp residues. The color of the residues in Fig. 3D shows how dynamic (based on RMSD) these residues are, with the red color indicating the most dynamic residues and the blue color the relatively less dynamic during the simulations.

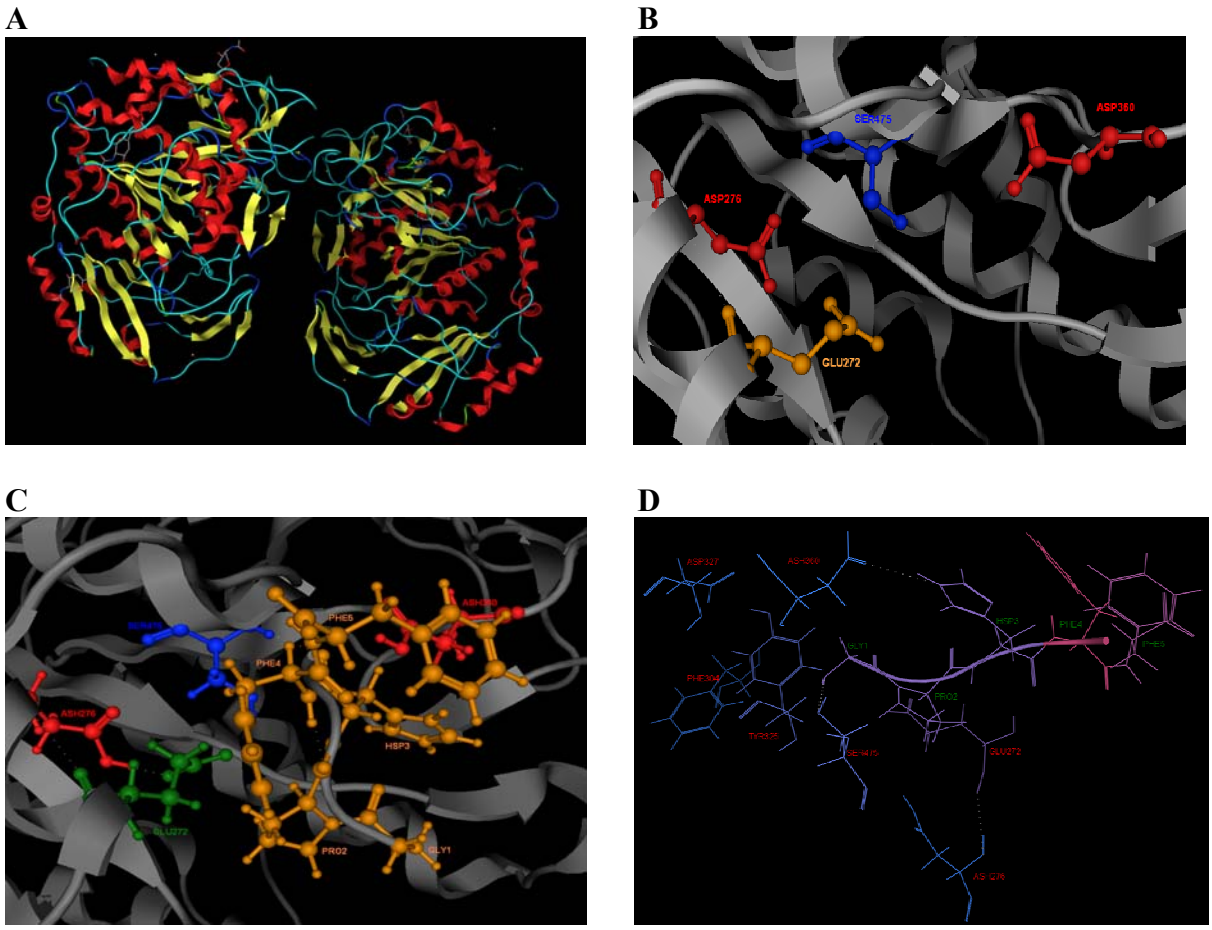


Fig.3. (A) 3-D Structure of the two chains of proenzyme TPP1 (PDB ID 3ee6) with α-helices and β-sheets colored in red and yellow, respectively. **(B)** The catalytic triad of the TPP1 (Ser475-Asp276-Glu272) and the also relevant Asp360, all them are important for the acid–base mechanism of acylation. **(C)** Structure of the catalytic triad and Ash360 with the 5-amino acid peptide (orange, ball and stick). Non-covalent H-bonding interactions are displayed. **(D)** Averaged structures and interactions after molecular dynamic simulations. Color represents differences in RMSD, being the red the most and the blue the less dynamic. Hydrogen-bonding interactions are observed between Ash360-Hsp3, Ser475-Gly1, and Ash276-Glu272. Protonated Asp is labeled as Ash.

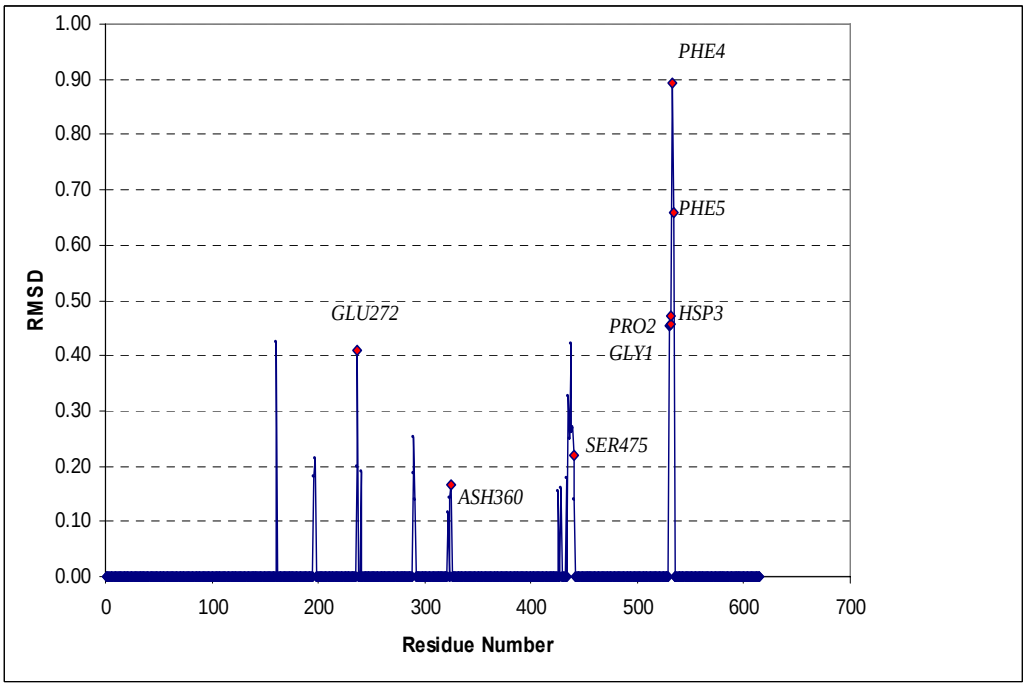


FIG.4. RMSD for the 5-amino acid substrate and surrounding residues (4.5Å). The peptide substrate (Gly1-Pro2-Hsp3-Phe4-Phe5) and relevant residues (Glu272, Ash360, Ser475) are labeled. Asp276 (not labeled) shows a lower RMSD of about zero.

The final outcome of the script using MOE shows a plot of RMSD against residue number to show the variation in position comparing system before and after the 4-ns dynamic simulation. The residues from the five-amino acid substrate show the highest RMSD values (Fig.4).

(iii) Discussion

MOE is very useful software that can help predict possible conformations and dynamics of residues through computer simulations. The 4-ns molecular dynamics

simulations provided information about the motion and position of the residues of interest as well as the change of the structure from the initial one after the dynamics simulation. The highest RMSD values correspond to the peptide substrate, suggesting that it may undergo significant changes in the conformations because the initial conformation is presumably unstable. Among the catalytic triad, Glu272 shows the highest RMSD value, followed by Ser475 and then Ash360. Three hydrogen-bond interactions involving Ash360- Hsp3, Ser475-Gly1, and Ash276-Glu272 were found to be stable after 4-ns simulations. No apparent stabilizing interactions are observed between Phe4/Phe5 and the key surrounding residues, and as a consequence, the last two residues from the substrate are more likely to be dynamic and have high RMSD values. The initial hydrogen bonding interactions in the constructed model (before running the 4-ns dynamics simulation) are between Ash276-Glu272 (two hydrogen bonds), Ser475-Hsp3, and Phe4-Pro2.

III. Computational Studies of Kumamolisin-As (Kum-As)

Kumamolisin-As (Kum-As) is an acid collagenase with a subtilisin-like fold. Its active site contains a unique catalytic triad, Ser278-Glu78-Asp82 (as in kumamolisin), and a putative transition-state stabilizing residue, Asp164.[17] Kum-As is a member of the sedosilin family identified by Tsuruoka *et al.* culture filtrate of a thermoacidophilic soil bacterium, *Alicyclobacillus sendaiensis* strain NTAP-1.[18, 19] Kum-As is encoded as a 57-kDa precursor protein consisting of an N-terminal prodomain and a catalytic domain.[17] The side chain residues from the catalytic triad (Ser278-Glu78-Asp82) are connected by hydrogen-bond interactions, which are extended out to two additional residues, Glu32 and Trp129.[4, 20] It is

important to note that kumamolisin is 93% identical with kumamolisin-As in its primary structure.[17] Kum-As is the first example of a collagenase from the sedolisin family (MEROPS53).[20] Collagen (~30% of the total weight of animal proteins) is an insoluble

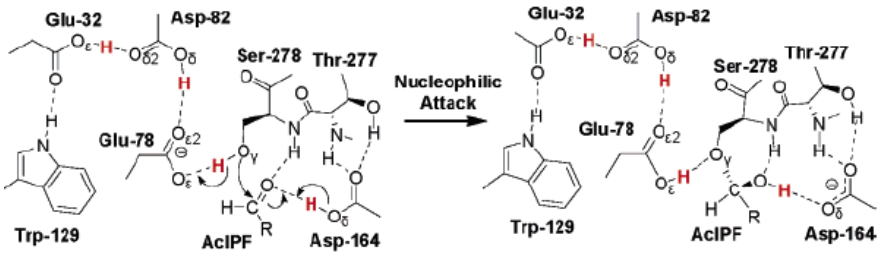


Fig.5. Suggested mechanism for the formation of the tetrahedral adduct (hemiacetal) from the aldehyde complex in the active site of kumamolisin-As by the nucleophilic attack of Ser278. Proton subject of this study are colored in red. Guo *et al.* 2006

structural protein predominant constituent of skin, cartilage and tendons; collagen provides the structure and strength in nearly all extracellular matrix of organs by being present in the connective tissue as insoluble fibers.[21]

As a sedolisin family member, the kumamolisin-As have a Ser-Glu-Asp catalytic triad (Ser278-Glu78-Asp82) and the presence of an aspartic acid residue (Asp164), a residue in charge of the creation of the oxyanion hole in classical serine proteases. An early study suggested that kumamolisin-As stabilizes the tetrahedral intermediates and adducts primarily through a general acid–base mechanism with Asn164 acting as a general acid catalyst to protonate the tetrahedral intermediate and assist in the nucleophilic attack by Ser278. The Glu78 next to Ser278 is likely to act as the general base to accept the proton from Ser278 (Fig.5).[22] 2D free energy map studies demonstrate that the proton transfer from Ser278 to Glu78 (the general base catalyst) is synchronous with the nucleophilic attack, whereas the proton transfer from Asp164 (the general acid catalyst) to the inhibitor is not.[23] This Asp

residue act as a general acid catalyst to stabilize the tetrahedral intermediate, leading to the rate acceleration for the enzyme-catalyzed reaction in contrast with the serine protease mechanism of electrostatic interactions of the oxyanion-hole used for stabilizing the tetrahedral intermediate during catalysis.[23]

In this thesis, the acylation reaction catalyzed by kumamolisin-As of the 5-peptide substrate is analyzed using quantum mechanical/molecular mechanical (QM/MM) molecular dynamics (MD) and free energy (potential of mean force) simulations.

(i) Methods

QM/MM molecular dynamics (MD) and free-energy (potential of mean force) simulations were performed using Chemistry and Harvard Molecular Mechanics (CHARMM) program with the semi-empirical density-functional method (SCC-DFTB). The initial coordinates for the X-ray crystal structures (pro-kumamolisin and kumamolisin-As) were obtained from the Protein Data Bank (ID: 1t1e and 1sio, respectively). The structures were superimposed, and the five amino acid peptide of the linker fragment from 1t1e was used to generate the substrate for kumamolisin-As leading to wild-type kumamolisin-As-substrate complex. A model of the D164N–substrate complex was also built by the superposition of the apo structure of D164N (Protein Data Bank ID: 1zvj) and the structure of pro-kumamolisin (ID:1t1e) in which the linker peptide GPHFF of 1t1e was used to generate the substrate. The models were optimized by using MOE software.

Protons were manually added to some ionizable residues to mimic the structures determined a low pH environment. The method of stochastic boundary, optimized by adopted basis Newton–Rhaphson (ABNR), was applied for the QM/MM simulations,

separating the system into the reservoir zone and the reaction zone. The latter was further separated into the reaction region and the buffer region. For the MM region, the all-hydrogen potential function (PARAM22) was used, to separate both the MM and the QM region, the link atom approach was employed. A modified TIP3P water model was used as solvent, and explicit water spheres covering the area of study were applied to solvate the systems. To determine the change of free energy for the acylation reaction of the kumamolisin wild type and single mutant, the umbrella sampling method and the Weighted Histogram Analysis Method (WHAM) were applied to this study.

(ii) Results and Discussion

Kum-As X-ray crystal structure shows the entire characteristics discussed above (Fig. 6B). All these features were analyzed using the useful tools in MOE to display residues. The average active site structure provides a better idea of the role of the catalytic triad, especially the nucleophile Ser278 (Fig. 6A)

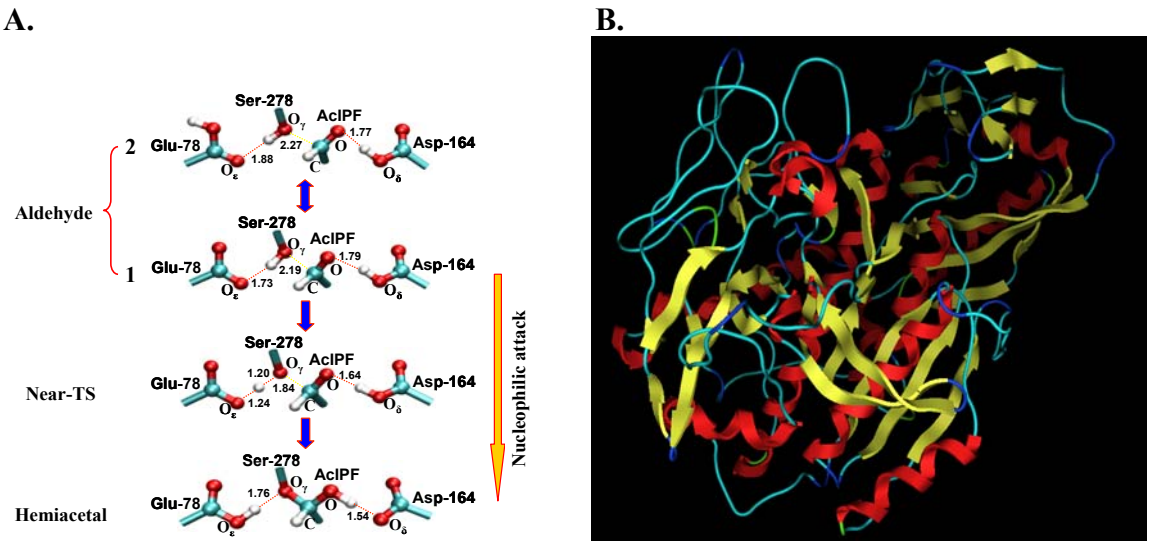


FIG.6. (A) Average active site structures for the atoms involved in nucleophilic attack in the aldehyde and hemiacetal complexes, Guo, H *et al.* 2006. **(B)** Pro-Kumamolisin secondary structure (PDB ID 1T1E)

The reaction coordinate [= r(C-N) – r(C-Oγ)] is the difference between the bond distance of the scissile peptide bond [r(C-N)] and the [r(Oγ(Ser278)-C)] distance of the nucleophilic attack during the acylation reaction. The free-energy plots in Fig. 7 show that the free-energy barrier of the acylation reaction is considerably lower for the wild-type Kum-As compared to that in the D164N mutant, which is consistent with experimental observations that the D164A mutant of kumamolisin (which is very similar to kumamolisin-As) did not show any measurable proteolytic activity.[4]

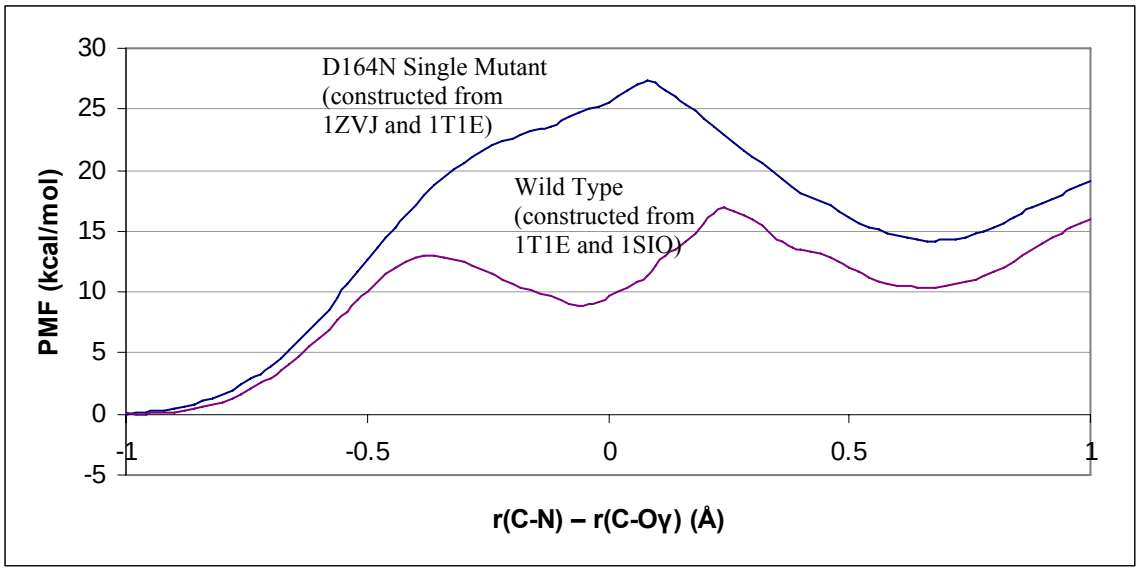


Fig.7. Free energy profiles of the acylation reaction for the wild-type kumamolisin-As and D164N single mutant as a function of the reaction coordinate [ξ= *r*(C-N) - *r*(C-Oγ] obtained from the QM/MM free energy (potential of mean force) simulations.

Asp164 seems to facilitate the acylation reaction, as it is demonstrated by the results of the simulations that the free-energy barrier increases significantly as a result of D164→N mutation. The proposed acid–base mechanism for stabilization of the reaction intermediates depends on the role of Asp164 as a general acid catalyst. This property is lost when D164 is mutated to Asn.

Conclusion

Understanding the structure and function of TPP1 is crucial for developing possible therapies and treatments against people with late neuronal ceroid lipofuscinosis that is a consequence of the mutation in the CLN2 gene that encodes for TPP1. New research advances are on their way, especially after the presence of new and more adequate X-ray

crystal structure data. The studies of TPP1, as well as the enzymes in the same family (e.g., Kum-As), could potentially increase the understanding of TPP1. QM/MM molecular dynamics simulation reveals the importance of D360 in TPP1 (and D164 in Kum-As) and its role as the acid–base catalyst for the acylation step.

Acknowledgements

Thanks to Dr. Hong Guo, Dr. Qin Xu and Dr. Haobo Guo for all of their contributions and discussions that made this study possible. In addition, thanks to Dr. Christopher Craig, Yuzhuo Chu, Barmak Mostofian, and Glenn Hernandez. I am grateful for the support and funds provided by the College Scholars Program and the Chancellor Honors.

References

1. Wlodawer, A.; Li, M.; Gustchina, A.; Oyama, H.; Dunn, B. M.; Oda, K. Structural and enzymatic properties of the sedolisin family of serine-carboxyl peptidases. *Acta Biochim. Pol.* **2003,** 50, 81-102.
2. Wlodawer, A.; Li, M.; Dauter, Z.; Gustchina, A.; Uchida, K.; Oyama, H.; Dunn, B. M.; Oda, K. Carboxyl proteinase from Pseudomonas defines a novel family of subtilisin-like enzymes. *Nat. Struct. Biol.* **2001,** 8, 442-446.
3. Wlodawer, A.; Li, M.; Gustchina, A.; Dauter, Z.; Uchida, K.; Oyama, H.; Goldfarb, N. E.; Dunn, B. M.; Oda, K. Inhibitor complexes of the Pseudomonas serine-carboxyl proteinase. *Biochemistry* **2001,** 40, 15602-15611.
4. Comellas-Bigler, M.; Fuentes-Prior, P.; Maskos, K.; Huber, R.; Oyama, H.; Uchida, K.; Dunn, B. M.; Oda, K.; Bode, W. The 1.4 angstrom crystal structure of kumamolysin: A thermostable serine-carboxyl-type proteinase. *Structure* **2002,** 10, 865-876.
5. Lin, L.; Sohar, I.; Lackland, H.; Lobel, P. The human CLN2 protein/tripeptidyl-peptidase I is a serine protease that autoactivates at acidic pH. *J. Biol. Chem.* **2001,** 276, 2249-2255.
6. Guhaniyogi, J.; Sohar, I.; Das, K.; Stock, A. M.; Lobel, P. Crystal structure and autoactivation pathway of the precursor form of human tripeptidyl-peptidase 1, the enzyme deficient in late infantile ceroid lipofuscinosis. In *The Journal of Biological Chemistry*, Piscataway, 2008.
7. Pal, A.; Kraetzner, R.; Gruene, T.; Grapp, M.; Schreiber, K.; Gronborg, M.; Urlaub, H.; Becker, S.; Asif, A. R.; Gartner, J.; Sheldrick, G. M.; Steinfeld, R. The Structure of Tripeptidyl Peptidase I provides insight into the molecular basis of late infantile neuronal ceroid lipofuscinosis. In *The Journal of Biological Chemistry*, Gottingen, 2008.
8. Page, A. E.; Fuller, K.; Chambers, T. J.; Warburton, M. J. PURIFICATION AND CHARACTERIZATION OF A TRIPEPTIDYL PEPTIDASE-I FROM HUMAN OSTEOCLASTOMAS - EVIDENCE FOR ITS ROLE IN BONE-RESORPTION. *Arch. Biochem. Biophys.* **1993,** 306, 354-359.
9. Lindas, A. C.; Eriksson, S.; Jozsa, E.; Tomkinson, B. Investigation of a role for Glu-331 and Glu-305 in substrate binding of tripeptidyl-peptidase II. *BBA-Proteins Proteomics* **2008,** 1784, 1899-1907.
10. Moser, H. W. Neurodystrophies and Neurolipidoses. *Handbook of Clinical Neurology* 1996, pp 671-700.
11. Rider, J. A.; Dawson, G.; Siakotos, A. N. In *PERSPECTIVE OF BIOCHEMICAL-RESEARCH IN THE NEURONAL CEROID-LIPOFUSCINOSIS*, 1992; Wiley-Liss: 1992; pp 519-524.
12. Cabrera-Salazar, M. A.; Roskelley, E. M.; Bu, J.; Hodges, B. L.; Yew, N.; Dodge, J. C.; Shihabuddin, L. S.; Sohar, I.; Sleat, D. E.; Scheule, R. K.; Davidson, B. L.; Cheng, S. H.; Lobel, P.; Passini, M. A. Timing of therapeutic intervention determines functional

and survival outcomes in a mouse model of late infantile batten disease. *Mol. Ther.* **2007,** 15, 1782-1788.
13. Sleat, D. E.; Donnelly, R. J.; Lackland, H.; Liu, C. G.; Sohar, I.; Pullarkat, R. K.; Lobel, P. Association of mutations in a lysosomal protein with classical late-infantile neuronal ceroid lipofuscinosis. *Science* **1997,** 277, 1802-1805.
14. Chang, C. H. Neuronal Ceroid Lipofuscinoses. http://emedicine.medscape.com/article/1178391-overview (January 4, 2009).
15. Worgall, S.; Sondhi, D.; Hackett, N. R.; Kosofsky, B.; Kekatpure, M. V.; Neyzi, N.; Dyke, J. P.; Ballon, D.; Heier, L.; Greenwald, B. M.; Christos, P.; Mazumdar, M.; Souweidane, M. M.; Kaplitt, M. G.; Crystal, R. G. Treatment of late infantile neuronal ceroid lipofuscinosis by CNS administration of a serotype 2 adeno-associated virus expressing CLN2 cDNA. *Hum. Gene Ther.* **2008,** 19, 463-474.
16. Chang, M.; Cooper, J. D.; Sleat, D. E.; Cheng, S. H.; Dodge, J. C.; Passini, M. A.; Lobel, P.; Davidson, B. L. Intraventricular enzyme replacement improves disease phenotypes in a mouse model of late infantile neuronal ceroid lipofuscinosis. *Mol. Ther.* **2008,** 16, 649-656.
17. Okubo, A.; Li, M.; Ashida, M.; Oyama, H.; Gustchina, A.; Oda, K.; Dunn, B. M.; Wlodawer, A.; Nakayama, T. Processing, catalytic activity and crystal structures of kumamolisin-As with an engineered active site. *Febs J.* **2006,** 273, 2563-2576.
18. Tsuruoka, N.; Isono, Y.; Shida, O.; Hemmi, H.; Nakayama, T.; Nishino, T. Alicyclobacillus sendaiensis sp nov., a novel acidophilic, slightly thermophilic species isolated from soil in Sendai, Japan. *Int. J. Syst. Evol. Microbiol.* **2003,** 53, 1081-1084.
19. Tsuruoka, N.; Nakayama, T.; Ashida, M.; Hemmi, H.; Nakao, M.; Minakata, H.; Oyama, H.; Oda, K.; Nishino, T. Collagenolytic serine-carboxyl proteinase from Alicyclobacillus sendaiensis strain NTAP-1: Purification, characterization, gene cloning, and heterologous expression. *Appl. Environ. Microbiol.* **2003,** 69, 162-169.
20. Wlodawer, A.; Li, M.; Gustchina, A.; Tsuruoka, N.; Ashida, M.; Minakata, H.; Oyama, H.; Oda, K.; Nishino, T.; Nakayama, T. Crystallographic and biochemical investigations of kumamolisin-As, a serine-carboxyl peptidase with collagenase activity. *J. Biol. Chem.* **2004,** 279, 21500-21510.
21. Harrington, D. J. Bacterial collagenases and collagen-degrading enzymes and their potential role in human disease. *Infect. Immun.* **1996,** 64, 1885-1891.
22. Guo, H. B.; Wlodawer, A.; Guo, H. A general acid-base mechanism for the stabilization of a tetrahedral adduct in a serine-carboxyl peptidase: A computational study. *J. Am. Chem. Soc.* **2005,** 127, 15662-15663.
23. Guo, H. B.; Wlodawer, A.; Nakayama, T.; Xu, Q.; Guo, H. Catalytic role of proton transfers in the formation of a tetrahedral adduct in a serine carboxyl peptidase. *Biochemistry* **2006,** 45, 9129-9137.